Revised Manuscript

DOI:
Full Paper

The influence of physicochemical properties of biomimetic hydroxyapatite on the in vitro behavior of endothelial progenitor cells and their interaction with mesenchymal stem cells

Joanna Maria Sadowska, Jordi Guillem-Marti, Maria-Pau Ginebra*

Dr. Joanna Maria Sadowska, Dr. Jordi Guillem-Marti, Prof. Maria-Pau Ginebra
Biomaterials, Biomechanics and Tissue Engineering Group
Department of Materials Science and Metallurgical Engineering
Universitat Politècnica de Catalunya (UPC)
EEBE
Av. Eduard Maristany 10-14, 08019 Barcelona, Spain.
E-mail: maria.pau.ginebra@upc.edu

Dr. Joanna Maria Sadowska, Dr. Jordi Guillem-Marti, Prof. Maria-Pau Ginebra
Barcelona Research Centre in Multiscale Science and Engineering
Universitat Politècnica de Catalunya (UPC)
EEBE
Av. Eduard Maristany 10-14, 08019 Barcelona, Spain

Prof. Maria-Pau Ginebra
Institute for Bioengineering of Catalonia (IBEC)
The Barcelona Institute of Science and Technology
Baldiri Reixac 10-12, 08028 Barcelona Spain.

Keywords: calcium phosphates, osteogenesis, angiogenesis, coculture

Calcium phosphate (CaP) substrates are successfully used as a bone grafts due to their osteogenic properties. However, the influence of the physicochemical features of CaPs in angiogenesis is frequently neglected despite it is a crucial process for bone regeneration. The present work focuses on analyzing the effect of textural parameters of biomimetic calcium deficient hydroxyapatite (CDHA) and sintered beta-tricalcium phosphate (β-TCP) such as specific surface area (SSA), surface roughness and microstructure on the behavior of rat endothelial progenitor cells (rEPCs) and their crosstalk with rat mesenchymal stem cells (rMSCs). The higher reactivity of CDHA resulted in low proliferation rates in mono- and cocultured systems. This effect was especially pronounced for rMSCs alone, and for CDHA

with fine microstructure. In terms of angiogenic and osteogenic gene expression, the upregulation of particular genes was especially enhanced for needle-like CDHA compared to plate-like CDHA and β-TCP suggesting the importance not only of chemistry of substrate but also its textural features. Moreover, the coculture of rEPCs and rMSCs on needle-like CDHA resulted in early upregulation of osteogenic modulator *i.e.* protein deglycase 1 (DJ 1) what might be a possible cause of overexpression of osteogenic- related genes on the same substrate.

1. Introduction

Bone healing is a complex process that involves multiple interdependent and overlapping-in-time steps.[1] For instance, the timely angiogenesis serves not only as a source of oxygen and nutrients, but also controls the recruitment and differentiation of stem cells, the osteoblastic activity and consequently further new bone formation.[2,3] Therefore, the interplay between vessel-forming endothelial cells (ECs) and bone-forming cells is critical during the bone healing process. The ability of these cells to communicate, both through autocrine/paracrine routes and through direct gap junctional cell-to-cell contacts, results in a tight coupling between angiogenesis and osteogenesis.[2] For instance, mesenchymal stem cells (MSCs) and osteoblasts secrete angiogenic factors such as vascular endothelial growth factor (VEGF),[4] fibroblasts growth factor (FGF)[5] and protein deglycase 1 (DJ 1)[6] whose goal is to enhance ECs proliferation and subsequent vessel growth. On the other hand, ECs express bone morphogenetic protein 2 (BMP-2) and endothelin 1 (EDH 1), which fulfil dual function by regulating angiogenesis as well as stimulating bone formation.[7–10]

Despite the remarkable self-regenerative capacity of bone tissue, large defects cannot be bridged unless some support structures, namely bone grafts, are implanted to support the healing process. Calcium phosphates (CaPs) have been shown to be excellent synthetic bone grafts, due to their close compositional resemblance to the mineral phase of bone. Furthermore, some of them such as sintered β-TCP or low temperature CDHA[11,12] were reported to possess osteoconductive/osteoinductive properties that might foster the osteogenesis-related processes.

Great efforts have been made in CaPs research towards investigating to which extent and how their particular physicochemical features such as macroporosity, chemistry, ionic release/uptake, and surface topography affect the osteoinductive/osteoconductive potential.[13,14] Nonetheless, since bone healing process is complex, involving not only bone-forming cells but also immune or endothelial cells, the implant should actively participate in the former stages of bone regeneration exhibiting anti-inflammatory and angiogenic properties as well as stimulating the proper crosstalk between the different cell types implicated in restoring of bone function.

Recently, some advances have been made in modulating the angiogenic performance of CaP-based materials. The macroporosity,[15,16] functionalisation/loading of scaffold with biomolecules like RGD[16] or VEGF[17,18] or incorporation of ions like cooper[19] or cobalt[20] have been investigated as strategies for potentiating the angiogenic features of CaPs. Moreover, the *in vitro* prevascularisation of bone grafts was also studied as an interesting approach for the preparation of constructs with enhanced angiogenic performance. For instance, Chen *et al.* and Thein-Han *et al.* showed that coculturing of endothelial and bone forming cells on microporous calcium phosphate scaffolds had positive impact on stimulating the formation of microcapillary network as well as the expression of genes involved in both angiogenesis and osteogenesis.[16,21] Although the pathways involved in activation of positive crosstalk of endothelial and bone cells have been widely investigated,[22,23] little attention has been paid to the effect of particular features of CaPs on the angiogenic and osteogenic events in coculture conditions.

Therefore, the current study tackles two main goals. The first was to investigate to which extent the particular cues of CDHA affect the behaviour of endothelial progenitor and mesenchymal stem cells separately. Two chemically identical biomimetic calcium deficient hydroxyapatite, consisting of either needle-like or plate-like crystals were compared to sintered β-TCP in terms of its effect on rEPCs and rMSCs proliferation, PECAM-1 production and osteogenic/angiogenic gene expression. As a second goal, the outcome of physicochemical features of CaPs on the interaction of rEPCs and rMSCs were investigated through coculture system evaluating angiogenic and osteogenic gene expression and the secretion of connexin43, a junctional protein responsible for cell-to-cell communication. Additionally, the expression of protein deglycase 1 (DJ 1) and endothelin 1 (EDH 1) was analysed, as possible mediators of rEPCs and rMScs crosstalk.

2. Results

2.1. Physicochemical characterization of CaPs

The XRD diffraction confirmed that CaPs are phase-pure (**Figure 1**C) except for C-CDHA, where traces of unreacted α- TCP were observed (< 3%). The sintered β-TCP showed sharp diffraction peaks whilst broad peaks were observed for C-CDHA and especially for F-CDHA substrates. Whereas all materials presented similar porosities (Figure 1D), clear differences were observed in terms of microstructure. C-CDHA consisted of plate-like crystals, whereas F-CDHA presented nanometric sized needle-like crystals, organised in agglomerates. The sintering process of β-TCP led to the formation of polyhedral crystals (Figure 1A). The microstructural differences resulted in higher SSA for the biomimetic CDHA compared to sintered β-TCP. C-CDHA presented higher average roughness values than F-CDHA and sintered β-TCP (1.33±0.23) (Figure 1B).

2.2. Initial adhesion and proliferation in monocultures and cocultures

Similar adhesion of monocultured rEPCs was observed in all substrates (**Figure 2**A). Monocultured rEPCs progressively increased their number in all CaPs with slightly slower proliferation rate on biomimetic CDHA substrates. Moreover, lower number of monocultured rEPCs on β-TCP at day 3 was observed compared to TCPS.

In monocultured rMSCs, the cellular adhesion was lower on CDHA substrates whilst β-TCP presented similar number of adhered cells compared to the control. Overall, the proliferative potential of monocultured rMSCs was lower when cultured on CaP substrates. This scenario was especially pronounced for biomimetic substrates where the cellular proliferation was significantly slowed down or impaired on C-CDHA and F-CDHA, respectively. Moreover, the β-TCP showed significantly lower number of monocultured rMSCs at day 21 compared to the control.

In coculture system, the cellular adhesion was also lower on CDHA compared to β-TCP and TCPS. The cells presented low proliferation rate on biomimetic CDHA being this scenario especially pronounced on F-CDHA, where similar cell numbers were observed over the cell culture times. Nonetheless, the proliferative potential of cells on C-CDHA was higher on coculture condition compared to monocultured rMSCs. The enhanced proliferation rate on coculture was also observed for β-TCP compared to monocultured rMSCs.

2.3. Ionic concentration

The evolution of calcium and phosphate concentration in the EGM-2 MV culture medium in presence of cells is displayed in Figure 2B and 3C, respectively. The initial value of Ca^{2+} concentration was 1.89±0.05 mM. In general, irrespective of the cell type, little alteration of calcium levels was observed for C-CDHA and β-TCP. In monocultured rEPCs, F-CDHA uptook Ca^{2+} ions from the medium, this resulting in a 20% decrease in calcium concentration compared to the control throughout the whole culture period. In rMSCs monoculture, the decrease of Ca^{2+} by F-CDHA was observed at 6 h and 14 d of cell culture whilst this trend for coculture was noted at 6 h, 14 and 21 d.

The initial experimental value of P_i was 1.02±0.01 mM. In general, higher P_i levels were detected in presence of the biomimetic substrates, whereas the values registered for the β-TCP substrates were similar to TCPS. Despite using the same cell culture medium, different trends were observed for the biomimetic substrates depending on cell type. For rEPCs monoculture, the CDHA increased approximately 50% the P_i concentration compared to TCPS at 6 hours. In contrast, for rMSCs monoculture and coculture on biomimetic CDHA highest levels of P_i were observed at day 3, reaching approximately 170% and 130% P_i concentration compared to TCPS, respectively. Comparing the two biomimetic substrates, F-CDHA led to more pronounced changes of Pi content. In all cell culture conditions on CDHA, slow and progressive decrease of Pi concentration was observed after reaching the aforementioned highest levels.

2.4. Cell morphology

Cellular morphology in mono- and coculture on CaP substrates at 14 and 21 days were studied through visualisation with a CLSM. For that purpose, cells were stained for F-actin and nuclei (**Figure 3**). In all conditions, the cells presented a spread morphology with well-defined cytoskeleton except for monocultured rMSCs on F-CDHA at day 21.

Cx43, a gap-junction protein, was visualised in all CaP substrates over all cell culture conditions at days 14 and 21 (**Figure 4**). The analysis revealed that Cx43 protein was mainly colocalised with F-actin in cells cultured on CaPs being this scenario similar to that observed in control group. In all conditions the presence of Cx43 was mainly localized in the outer part of the cellular membrane.

In order to distinguish rEPCs at coculture conditions, cells were additionally incubated with endothelial specific PECAM-1 and compared to monocultured rEPCs (**Figure 5**A). Whilst PECAM-1 was well visible in rEPCs monoculture, a small number of PECAM-1 positively stained cells were observed in coculture. Semiquantitative analysis of CLSM images revealed that at day 14 the PECAM-1 stained area in rEPCs monoculture was slightly lower on C-CDHA and β-TCP sample whilst the F-CDHA showed similar values to that observed on control group (Figure 5B). In case of coculture, increased values of PECAM-1 stained area were observed for C-CDHA at day 14 (Figure 5C) compared to other CaPs and control. These differences between substrates were not statistically significant and they disappeared at day 21.

2.6. Gene expression

2.6.1. Osteogenic gene expression

The expression of genes related to osteogenesis is depicted in **Figure 6**. In general, an upregulation of the osteogenic genes was detected on the CaP substrates, both in mono- and coculture conditions. A considerable upregulation of the ALP expression was observed on the F-CDHA substrate, irrespective of cell type. In monocultured rMSCs the maximum value was attained at day 1, decreasing at 7 and 14 days. In contrast, in monocultured rEPCs and in the cocultures the ALP expression increased at 1 and 7 days, strongly decreasing at day 14. The expression of BMP-2 was higher for monocultured rEPCs compared to the other culture conditions in all substrates at day 1, decreasing afterwards. Conversely, monocultured rMSCs and coculture continuously increased their BMP-2 expression until day 7, especially for F-CDHA, and they maintained similar levels at day 14 irrespective of the substrate. Regarding

OC expression, it was upregulated at early time points in the rEPCs, whilst in rMSCs and coculture the increase was shifted to 7 or 14 days. Moreover, the upregulation was higher on F-CDHA substrate in comparison to the other CaPs, irrespective of the cell type. The expression levels of DJ 1were higher in the two CDHA substrates compared to β-TCP. These levels were especially high in monocultured rEPCs and coculture at day 1 in both C-CDHA and F-CDHA. Subsequently, they decreased in all substrates except for rEPCs cultured on F-CDHA. Monocultured rMSCs on C-CDHA showed also a high upregulation at day 7.

2.6.2. Angiogenic gene expression

The expression of angiogenic markers is depicted in **Figure 7**. VEGF A was overexpressed by cells cultured on F-CDHA at all time points, especially by rEPCs but also in the 1:2 rEPCs:rMSCs cocultures an in the rMSC monocultures. In contrast, the cells cultured on C-CDHA and sintered β-TCP produced similar VEGF A expression pattern: an initial peak at day 1, followed by a brusque decrease at days 7 and 14. The expression profile of VEGF R2 was strongly dependent of cell type and substrate, although an overexpression was observed on all CaP substrates. In general, biomimetic substrates showed to cause more fluctuations in VEGF R2 expression rather than sintered β-TCP, which maintained similar VEGF R2 values over cell culture. For biomimetic CaPs, the overexpression of VEGF R2 was mainly observed in rEPCs monoculture presenting the highest values at days 7 and 14 for C-CDHA and F-CDHA, respectively. The expression of EDH 1 was strongly enhanced by F-CDHA at day 1 and 7 for rEPCs monoculture and at day 14 for coculture. In contrast, overexpression of EDH1 was observed in the rEPCs monoculture on β-TCP at day 14.

2.6.3. The effect of rEPCs and rMSCs coculture on osteogenic and angiogenic gene expression

The effect of coculture on the expression of osteogenic and angiogenic markers is presented in **Figure 8**. Upregulation of osteogenic markers in coculture condition was substrate and gene dependent. In general, the F-CDHA substrate led to higher values of upregulation of osteo-specific genes compared to other biomimetic C-CDHA and to sintered β-TCP. For F-CDHA, the main upregulation peak of osteogenic genes was detected at day 1 or day 7 of coculture. Both biomimetic C-CDHA and sintered β-TCP showed similar patterns for BMP-2, OC and DJ 1 showing dual upregulation peak at day 1 and 14.

With regards to angiogenic gene expression, the cocultue of rEPCs and rMSCs resulted in strong upregulation of VEGF R2 and EDH 1 when the cells were cultured on F-CDHA and β-TCP, mainly at day 14 of coculture. The expression of EDH 1 was enhanced by F-CDHA whilst VEGF R2 expression was upregulated by both F-CDHA and β-TCP substrates (Figure 8).

3. Discussion

3.1. Proliferation of rEPCs and rMSCs on the different substrates

The proliferation of rEPCs and rMSCs was clearly affected by the substrate to different extents, being slower in general on the biomimetic CDHA (Figure 2A). The reduction of the proliferation rate was more pronounced for the rMSCs and the cocultures, particularly on F-CDHA. This can be attributed to various factors. For instance, medium composition, surface topography as well as the ratio between cell types in coculture system were reported to influence cell proliferation.[24–26] Following previous reports, we decided to use EGM-2 MV, a medium for the culture of endothelial cells, both for coculture and monocultures instead of a mixture of cell culture media to guarantee endothelial cell survival.[21,27–29] Even if the use of endothelial cell culture medium for rMSCs monoculture is not a common choice, several studies have demonstrated little effects on phenotypic features of MSCs when cultured in

EGM-2.[30–32] Moreover, the use of the same culture medium for all cultures is a clear advantage when comparing bioactive materials, which are known to interact with the cell culture medium. Using a single cell culture medium allows discarding any interactions due to the interaction of the material with the cell culture media of different compositions.

The analysis of cell behaviour on CaP substrates requires to take into consideration not only their physicochemical features but also their intrinsic reactivity with aqueous environment. The reactive behaviour of CaPs *in vitro* and its further effect on bone cell behaviour, more pronounced for substrates with high SSA, has been widely reported.[13,33–35] For instance, we previously showed that CDHA altered ionic concentration to a higher extent than sintered ceramics[36], which can be related not only to the high SSA, but also to the presence of non-apatitic domains on their crystal surface.[37,38] Moreover, the distinct structural features of chemically identical substrates used in the present study, *i.e.* F-CDHA and C-CDHA, might produce different ionic fluctuations and thereby affect the cellular behaviour to different extents. Another interesting issue is that expected ionic fluctuations might vary depending of medium composition[34,36] as well as presence or not of cells[39]. In the latter case, the layer of cells might reduce the exposure of the substrate to different extents depending on the degree of surface coverage, which in turn would decrease the ionic exchange.[40] In the current study we observed that CDHA substrates released P_i , and in agreement with a previous work,[41] this trend was more pronounced for F-CDHA than for C-CDHA, due to its higher SSA. This behaviour can be associated with the incorporation of B-type carbonate into the apatite lattice, replacing phosphate groups, as demonstrated in a previous study.[41] In fact, the release of P_i also occured in absence of cells, as displayed in Figure S2.

Interestingly, although the monocultures and coculture on CaPs were performed using the same cell culture medium, the release of P_i was different in the different cultures. While the trends of P_i release observed for biomimetic substrates with monocultured rMSCs and coculture were simimilar to those without cells, the monocultured rEPCs decreased the P_i

release 2-fold for both F-CDHA and C-CDHA. However, since little differences of cellular adhesion on the biomimetic CDHA were observed at 6 hours of cell culture, the different P_i release cannot be explained with the hypothesis that the layer of cells might cover the surface of substrate reducing the ionic exchange.[40] Therefore, the different ionic behaviour observed in monocultured rEPCs could be attributed to the cellular activity. For instance, the endothelial cells exhibit the capacity to uptake P_i in hyperphosphatemia what increases the apoptosis rate.[42,43]

On another hand, given the calcium- defficient nature of CDHA substrates, an uptake of calcium from the cell culture medium triggered by the maturation of hydroxyapatite was expected, as proved in previous works usong other cell culture media.[41] However, little depletion of this ion was observed. This can be explained by the high Mg^{+2} content in the EGM-2 MV culture medium, which resulted in the uptake of this ion by the substrate, which likely mitigated the uptake of calcium, as shown in Figure S2.

In our study, monocultured rEPCs showed similar proliferative potential on all CaPs with slightly lower proliferation rate for biomimetic substrates (Figure 2 and 3). Previous studies with bioinert substrates showed that topographical cues of biomaterials have little impact on proliferation of endothelial cells.[44] For instance, Xu *et al.* observed similar adhesion and proliferation of ECs cultured on randomly electrospun PLLA substrates with either nano- or micro-roughness.[44] It is important to highlight that, unlike in the case of inert materials, calcium phosphates control cellular behaviour also through fluid-mediated effects *i.e.* the ionic exchange with cell culture medium. For instance, the depletion of magnesium in case of biomimetic CDHA (Figure S2) may result in the lower proliferative potential of monocultured rEPCs, since this particular ion was reported to be vital in modulating endothelial cell behaviour.[45,46] Other possible explenation for slowed proliferation of rEPCs on these substrates might be an uptake of P_i by cells what in turn results in apoptosis.[42,43]

In contrast, reduced proliferation was observed for biomimetic substrates in comparison to β-TCP in rMSCs monoculture. This might be attributed to two simultaneously affecting factors: the microstructure of CDHA and its intrinsic ionic reactivity. We previously demonstrated that ionic fluctuations caused by CDHA particularly affect rMSCs causing a reduction on the number of focal adhesions and cell shrinkage and leading to cell death via apoptosis.[36,41] Interestingly, although the F-CDHA possesses the same chemical composition as C-CDHA, it led to a more pronounced reduction of MSCs number. A similar behaviour was previously observed for osteoblastic cells.[47] The more pronounced release of P_i caused by F-CDHA due to its smaller crystal size and thus the higher SSA could be the responsible for this reduced proliferation. For instance, Liu *et al.* demonstrated that even small changes of P_i concentrations in cell culture medium reduce the proliferation of MSCs.[48] The effect of topography on cellular proliferation cannot be overlooked. For instance, we previously demonstrated that the contact of cells with topography of CaP substrate slowed down the proliferation rate compared to cells exposed exclusively to CaP extracts without the additional effect of microstructure.[36]

Slowed cell proliferation on coculture system was also observed for CDHA, also especially for F-CDHA. Since the greater part of cells was constituted of rMSCs, we hypothesize that this behavior can be also attributed to microstructure and ionic fluctuations of CDHA as above described for the rMSCs monoculture. Interestingly, the PECAM-1 staining revealed few number of rEPCs in coculture system, irrespective of the substrate (Figure 5). The possible explanation of this scenario might be the growth rate of cells that might change when exposed to coculture conditions.[24] Bidarra *et al.* showed that MSCs and ECs cultured alone exhibited different proliferation rate as when they were cocultured. The authors observed that ECs stimulated the expansion of MSCs what might contribute to curtail ECs capability to grow in coculture. This led to lower proliferation rate for EC in coculture compared to EC in monolayer what was also observed in our study.[24] Similarly, Fuchs *et al.* demonstrated low proliferative potential of ongrowth endothelial cells (OECs) when exposed to coculture conditions. Coculturing bone cells with OECs at ratio 3:2 lead to two opposite behaviors: whilst bone cells increased their number over time, a decrease was observed for OECs.[47] In our study, the low number of rECPs was interestingly observed in both CaPs and control group (Figure 5). The high proliferation rate of coculture for control group and β-TCP combined with low number of PECAM-1 positively stained cells suggest an increased growth of MSCs what might contribute to curtail effect over rEPCs (Figure 2A). Instead, the low cellular number of coculture observed on CDHA substrates suggests other parameters involved in reducing the rEPCs proliferation since this cannot be associated with increased rate of rMSCs proliferation. One possible explanation for this scenario might be the increased levels of phosphate from CDHA, since levels above 2.5 mM were reported to induce apoptosis in ECs.[43,50]

3.2. Angiogenic differentiation of rEPCs and rMSCs on the different substrates

In order to evaluate the angiogenic potential of CaPs, the expression of VEGF A and VEGF R2 was measured in mono- and coculture conditions (Figure 7). Additionally, cell cultures were subjected to the endothelial specific PECAM-1 staining to reveal wether rEPCs form microcapillary-like structures on CaP substrates (Figure 5).

VEGF A plays a pivotal role in the angiogenesis process, regulating the recruitment of endothelial progenitor cells as well as promoting its proliferation and differentiation.[23] VEGF A has been also suggested to mediate the secretion of osteogenic factors such as BMP-2, thus stimulating bone cell behaviour.[51] Interestingly, VEGF A is known to be expressed not only by endothelial cells, but also by pre-osteoblasts during differentiation,[52] thereby paracrinely stimulating angiogenesis. In our study, early VEGF A overexpression at 1 day was found when rEPCs were cultured on biomimetic substrates, notably more pronounced on

F-CDHA (Figure 7). Whilst rEPCs cultured on C-CDHA showed a decrease of VEGF A after 1 day expression peak, rEPCs on F-CDHA sustained high values of VEGF A. Furthermore, VEGF A expression was also upregulated for monocultured rMSCs and coculture on F-CDHA. This behaviour was not observed for other CaP substrates. Several authors studied the effect of bioactive character of substrates such as bioglasses on high expression of VEGF A in endothelial cells. However, they rather point the stimulatory effect of the release of calcium, which was not altered in our study.[53,54] On the other hand, the surface roughness also plays an important role in regulating angiogenic gene expression. For instance, the upregulation of VEGF A was observed in bioinert materials with surface roughness (Ra) of approximately 2 μm.[55] Although the bioactive character of CDHA hinder to interrelate the enhanced VEGF A expression with the topography of the substrate, we hypothesize that the roughness of CDHA might contribute to present scenario. The expression of VEGFR2 as the main receptor and major mediator of the angiogenic effects of VEGF on endothelial cells[56,57] was also studied. We found that the enhanced expression of VEGF A from endothelial cells cultured on F-CDHA substrate correlated with higher levels of their VEGFR2 at early time of cell culture. Interestingly, strongly enhanced values of VEGF A at 1 day for monocultured rEPCs on F-CDHA (Figure 7) also corresponded in time with upregulation of EDH 1 and DJ 1 (Figure 6) as well as sustained expression of BMP-2 (Figure 6)- potent angiogenic inducers.[8,58] Hence, we hypothesize that greater expression of VEGF A might be coupled with combined effect of the enhanced expression of these genes as well as upregulation of VEGF R2. For instance, Kim *et al*. demonstrated a positive effect of DJ 1 on VEGF A expression in endothelial cells through involvement of autocrine and paracrine mechanisms.[6]

Positively PECAM-1 stained cells were observed in both monocultured rEPCs and cocultured conditions (Figure 5A). Nevertheless, we did not observe capillary-like networks in any of the studied CaP substrate. In both mono- and coculture conditions rEPCs were present in the form of patches rather than showing aligned morphology.

3.3. Osteogenic differentiation of rEPCs and rMSCs on the different substrates

The commitment of mono and cocultured rEPCs and rMSCs towards osteoblastic lineage was also evaluated through RT-qPCR. Alkaline phosphatase (ALP) expression and osteocalcin (OC) are commonly used markers of early and late osteogenic gene expression, respectively. Whilst ALP is implicated in the regulation of local concentrations of inorganic phosphates fostering the mineralization,[59] OC regulates the quality and size of newly-formed mineral crystals.[60] Since the number of rMSCs on the different substrates was relatively low during all the cell culture time points, we were not able to measure the ALP activity. The gene expression of BMP-2 and DJ 1 were also evaluated since both participate in osteogenesis process as well as they are potent enhancers of angiogenesis.[6,61,62]

Different trends of expression of ALP, OC, BMP-2 and DJ 1 were observed for mono and coculture conditions (Figure 6). Moreover, the expression of each individual osteogenic marker was also time- and substrate-dependent. In general, cells cultured on CaPs materials showed higher gene expression at early time point compared to TCPS. This effect was observed for both mono- and coculture condition being more pronounced for biomimetic substrates. The result is coincident with other studies where stimulatory effect of CaPs on osteogenic expression was demonstrated.[41,63] For instance, we previously reported that biomimetic materials induce the differentiation of MSCs to greater extent than sintered ceramic.[36] This stimulatory effect is likely due to the coupled effect of subtle ionic fluctuations and surface topography- pivotal parameters in controlling osteogenic cell commitment.[64,65] The little changes of calcium content in EGM-2 MV medium after immersion of CDHA allowed the cell survival and further differentiation. This agrees with our previous finding where differentiation of MSCs into osteoblastic lineage cultured on CDHA was observed only when great ionic changes were mitigated. Interestingly, although both biomimetic CDHA own the same chemistry, the osteogenic differentiation was more pronounced for needle-like F-CDHA substrate suggesting the important role of surface topography.[47] This scenario, indeed, might contribute to curtail proliferation rate of MSCs (Figure 2A) inasmuch as osteogenic differentiation is usually accompanied by slower cellular proliferation.

3.4. Angiogenic and osteogenic differentiation of rEPCs and rMSCs in coculture

The impact of coculturing rEPCs with rMSCs on angio- and osteogenesis was depicted in Figure 8. Overall, the F-CDHA stimulated to a greater extent the gene expression in coculture conditions compared to rMSCs monocultured on the same substrate. Interestingly, this upregulation was more pronounced for osteogenic-related genes, which were upregulated either at 1 day (BMP-2, OC and DJ1) or 7 days (ALP and OC) (Figure 8). Regarding the angiogenic gene expression, there were no impact of coculturing rEPCs and rMSCs on upregulation of VEGF A, the main regulator of angiogenic events, on any of studied CaP substrates.

The previous reports showed that there are several parameters that might orchestrate this behavior in coculture. For instance, Villars *et al.* underlined that a direct cell contact, through gap junctional proteins like Cx43, is a fundamental condition for stimulation of gene expression in endothelial and bone cells in *in vitro* coculture systems.[66] However, since monocultured and cocultured cells presented similar secretion of Cx43 (Figure 4), the enhanced expression of osteogenic genes for coculture on F-CDHA should be attributed to other events that orchestrate this behavior. The great influence of potent osteogenic enhancers like BMP-2, EDH 1 and DJ 1 was also mentioned in literature. Kaigler *et al.* demonstrated that direct cell-cell contact mediate BMP-2 signaling from endothelial cells enhancing the ALP activity and OCN production of bone cells.[67] The effect of EDH 1, although frequently associated only with angiogenic events, was also reported to stimulate differentiation of osteoprogenitor cells.[23] Moreover, previous reports demonstrated that DJ 1 not only mediates the endothelial- bone cells' crosstalk but also induces osteogenesis through FGFR-1 signaling.[6] Since no enhanced expression of BMP-2 and EDH 1 in coculture was observed for F-CDHA substrate we hypothesize that the higher levels of DJ 1 might contribute to the osteogenic potential of F-CDHA.

4. Conclusion

The results demonstrate that distinct chemical features of CaPs substrate trigger various cell responses in terms of proliferation as well as angiogenic and osteogenic gene expression. In general, ionically more reactive CDHA affect proliferation rate to greater extent than sintered β-TCP. The F-CDHA led to more pronounced ionic changes than C-CDHA significantly reducing proliferation rate of rMSCs and the coculture of rECPs: rMSCs. For β-TCP, where cells were exposed to little ionic exchange, the coculture resulted in enhanced growth of rMSCs compared to monocultured rMSCs.

With regards to coculture condition, the cellular crosstalk was not reflected in enhanced secretion of gap junctional protein Cx43 but through upregulation of osteogenic-related genes. This behavior was mainly observed for F-CDHA substrate and might be related to enhanced expression of osteogenic inducer DJ 1.

5. Experimental Section

Determination of coculture ratio of rEPCs and rMSCs: For the coculture studies, both cell types were expanded separately in their corresponding cell culture media till 70-80% of confluence. Afterwards, rEPCs and rMSCs were detached and seeded at rEPCs:rMSCs ratios of 1:0, 4:1, 2:1, 1:1, 1:2, 1:4 and 0:1 onto 24-well plates. Cells were cultured up to 21 days in

EGM-2 MV medium at 37 ^{o}C in a humidified 5% CO_2 incubator replacing the medium every other day. The optimum ratio for coculture conditions was chosen evaluating cell proliferation, cell differentiation, and cell mineralization. The details regarding methods applied for quantification of cellular behaviour in coculture conditios were provided in Supplementary Information.

Material preparation: CDHA was obtained by hydrolysis of α- tricalcium phosphate (α-TCP) via a cementitious reaction, as previously described.[68] Briefly, α-TCP powder was prepared by heating at 1400°C for 15 h a 2:1 molar mixture of calcium hydrogen phosphate ($CaHPO_4$, Sigma-Aldrich, St. Louis, USA) and calcium carbonate ($CaCO_3$, Sigma-Aldrich, St. Louis, USA), followed by quenching in air. α-TCP powders with two different sizes were obtained by milling according to two different protocols. The α-TCP powder with larger size (coarse, C: 5.2µm median size) was obtained my milling in agate ball mill (Pulverisette 6, Fritsch GmbB) with 10 balls (d=30 mm) for 15 min at 450 rpm. The α-TCP powder with smaller size (fine, F: 2.8 µm) was first milled with 10 balls (d=30 mm) for 60 min at 450 rpm followed by second milling with 10 balls (d=30 mm) for 40 min at 500 rpm and the third one with 100 balls (d=10 mm) for 60 min at 500 rpm.[69]

CDHA discs were obtained by mixing a solid phase consisting of α-TCP powder and 2 wt.% of precipitated hydroxyapatite (PHA; Merck 2143, Merck, Darmstardt, Germany) with a liquid phase of 2.5 wt.% disodium hydrogen phosphate (Na_2HPO_4, Merck, Darmstadt, Germany), with a liquid to powder ratio of 0.35 mL g^{-1}. The paste was transferred to Teflon moulds (15 mm diameter and 2 mm thickness) and immersed in water at 37 ^{o}C for 7 days for complete reaction. The products obtained were coded as C-CDHA or F-CDHA depending on the size of the starting powder.

β-tricalcium phosphate discs were obtained by sintering C-CDHA at 1100^{o}C for 15 hours, followed by slow cooling inside the furnace.

Material characterization: Phase composition of the different CaPs was assessed by X-ray diffraction (XRD, D8 Advance, Brucker, Karlsruhe, Germany). The diffractometer equipped with a Cu Kα X-ray anode was operated at 40 kV and 40 mA. The data was collected in 0.02° steps over the 2θ range of 10°-80° with a counting time of 4s per step. The phases were identified by comparison to the diffraction patterns of HA (JCPDS 82-1943), α-TCP (JCPDS 09-0348) and β-TCP (JCPDS 70-2065). Semiquantitative XRD analysis of the products was carried out using the reference intensity ratio method.[70] The microstructure of materials was analyzed by Scanning Electron Microscopy (SEM, Zeiss Neon 40, Oberkochen, Germany) at an acceleration voltage of 5 kV. To impart conductivity, surfaces were coated with gold-palladium layer prior to imaging. The surface roughness was characterized by optical interferometry (Veeco Wyko NT1100), using a 50x magnification and a scanned area of 47.5 x 63.4 μm^2. Images were acquired using Vision32 software. The SSA and porosity of materials used in current study was described in previous reports.[71]

Cell culture study: The protocol of isolation of rat mesenchymal stem cells (rMSCs) and rat endothelial progenitor cells (rEPCs) was described elsewhere.[72] Briefly, cells were obtained from the tibias and femurs of Lewis rats at the Institute for Bioengineering of Catalonia (IBEC). Flow cytometry was performed in order to assess cell phenotype.[73]

rMSCs were grown in Advanced Dulbecco's Modified Eagle Medium (AdvDMEM) supplemented with 10% of foetal bovine serum (FBS), 2 mM L-glutamine, penicillin/streptomycin (50 U mL^{-1} and 50 µg mL^{-1}, respectively) and 20mM 4-(2-hydroxyethyl)-1-piperazineethanesulfonic acid (HEPES) buffer, provided from Invitrogen.

rEPCs were expanded in microvascular endothelial cell medium 2 (EGM2-MV, Lonza) containing endothelial cell basal medium (EBM-2, Lonza) supplemented with EGM-2 bullet kit and 5% FBS.

All experiments, except where stated, were performed with a seeding density of 12×10^3 cells per well using rMSCs and rEPCs at passages 3-5.

Monoculture and coculture of rEPCs and rMSCs on CaPs: C-CDHA, F-CDHA and β-TCP discs (12-15 mm of diameter, 2 mm of height) were sterilised with 70% ethanol, rinsed with PBS and pre- incubated overnight with complete EGM-2 MV medium at 37 ºC. Subsequently the corresponding cells were seeded on the substrates. The ratio 1:2 was used for coculture condition on discs considering the results obtained in the previous study. For both coculture[64] and monoculture of rEPCs and rMSCs,[31] EGM-2 MV medium was used. In all assays, the medium was refreshed after 6 hours of cell adhesion and then every other day throughout the whole culture period. Tissue culture polystyrene (TCPS) was used as corresponding control for each culture/co-culture condition. Cell number was evaluated at 6 hours, 3, 7, 14 and 21 days by measuring LDH activity following the previously detailed protocol (See Supporting Information). In order to express the absorbances' values as a cell number, individual calibration curves with a decreasing number of cells was prepared for each condtion *i.e.* rEPCs monoculture, rMSCs monoculture and 1:2 rEPCs:rMSCs coculture. For cells cultured on CaPs discs, results were normalised versus the area of the discs and then expressed as relative fold to TCPS at 6h.

Ionic concentration of cell culture media: At specific time points, the supernatants from mono- and cocultures on CaPs were collected and stored at -20 ºC for further analysis. Subsequently, the concentration of calcium and phosphorus were determined. The Ca^{2+} was quantified applying o- cresolphthalein complexone method.[74,75] The concentration of P_i was evaluated by Phosphate Colorimetric Assay Kit (Sigma- Aldrich) measuring the absorbance at 650 nm with Synergy HTX multi-mode microplate reader (Bio-Tek Instruments, Inc.). The changes in concentrations of calcium and phosphate for CaP substrates immersed in EGM-2 MV medium was also monitored without presence of cells up to 14 days. Since CDHA might also uptake other ions[41], the content of magnesium was additionally determined through Inductively Coupled Plasma Optical Emission Spectrometry (ICP-OES, 5100 ICP-OES, Agilent). Prior to quantification, the supernatants was diluted 20-fold with 2% of ultrapure nitric acid (Sigma-Aldrich).

Immunostaining: Monocultured rEPCs, rMSCs and coculture were stained for nuclei, F-actin and Connexin43 (Cx43). Monocultured rEPCs and coculture were additionally incubated with endothelial specific platelet endothelial cell adhesion molecule (PECAM-1, CD31). The staining was performed at 14 days and 21 days of cell culture. The samples were rinsed with PBS (x3) and cells were fixed with 4% (v/v) PFA solution in PBS. Afterwards, the permeablization process was carried out with 0.1 % Triton X- 100 (Sigma-Aldrich) in PBS during 15 min. Subsequently, cells were incubated 30 min at RT with blocking solution consisting of 1% bovine serum albumin (BSA) (Sigma-Aldrich) in PBS. The discs were incubated with the primary antibody rabbit anti- PECAM-1 (Santa Cruz Biotechnologies) at 1:100 in 1% BSA in PBS for one hour. The step was followed by incubation with secondary antibody Alexa Fluor 488 chicken anti- rabbit (1:1000) and Alexa Fluor 546 Phalloidin (1:300) in 0.1% Triton X- 100 in PBS (all from Invitrogen). For nuclei staining, 4',6-diamidino-2-phenylindole (DAPI) (1:1000 in 0.15% glycine in PBS) was added and samples were incubated for 2 minutes. Between all steps, three rinses for 5 minutes with 0.15% glycine (Sigma-Aldrich) in PBS were performed. For Cx43 staining the manufacturer instructions was followed in terms of cell fixation, dilution and incubation times. The primary antibody was mouse-anti Connexin43 C terminus (Millipore) and the secondary antibody was Alexa Fluor 488 goat anti- mouse (Invitrogen). The cells seeded on glass coverslip were used as a control group. Samples were mounted with Mowiol 4-88 (Sigma- Aldrich) and visualised using inverted LSM 800 ZEISS confocal microscope (CLSM). Images were acquired using LASX software and processed using Fiji/Image-J package.

Angiogenic ans osteogenic gene expression of cocultured rEPCs and rMSCs on CaPs: Angiogenic and osteogenic gene expression was evaluated at 1, 7 and 14 days of mono- and cocultures by quantitative real-time polymerase chain reaction (RT-qPCR).Total RNA was extracted from mono and cocultures at the given time points using RNeasy® Mini Kit (Qiagen, Hilden, Germany) as recommended by the manufacturer. Total RNA quantity was determined by NanoDrop ND-1000 spectrophotometer (NanoDrop Technologies, Montchanin, DE, USA) and subsequently 130 ng of the total RNA were used as template for single strand complementary DNA (cDNA) synthesis using QuantiTect Reverse Transcription Kit (Qiagen). Quantitative real-time PCR (RT- qPCR) assays were performed and monitored in triplicate using a StepOnePlus Real-Time PCR System (Applied Biosystems, Foster City, CA, USA). The cDNA template was amplified with the QuantiTect SYBR Green RT-PCR Kit (Qiagen) and specific primers for angiogenic and osteogenic markers (Listed in Table S1). No-RNA control, the melt curve analysis and no-RT control were run to ensure the specificity of primers and the absence of genomic DNA, respectively. The expression of all studied genes were normalized by expression of β-actin (ACTB) and relative fold changes (FC) were related to 1 day gene expression value of either rEPCs monocultured on TCPS with EGM-2 MV (for angiogenesis markers: VEGF A, VEGF R2, endothelin-1) or rMSCs monocultured on TCPS with advDMEM (for osteogenic markers: ALP, BMP-2, OC, DJ 1). The fold change was calculated with the formula

$$FC = E_{target}^{\Delta Cq\ target\ (TCPS\ 6h - sample)} / E_{reference}^{\Delta Cq\ reference\ (TCPS\ 6h - sample)}. \quad (1)$$

Cq respresents the median value of the quantification cycle of the triplicate of each sample. E corresponds to the efficiency of amplification and is determined through following formula $E = 10^{[-1/slope]}$ where slope value proceeds from slope of the log-linear portion of the calibration-curve.

Statistical analysis: Each experiment was performed in two independent runs except for the immunostaining and ionic content without presence of cells for which one experiment was performed for n=2 and n=3, respectively. Proliferation, ionic content in presence of cells and gene expression data were plotted as means ± SE with n=6. PECAM1 area was plotted as means ± SE with n=10. Normality was checked through the Saphiro–Wilk test. Statistical significance was determined by ANOVA with Tukey HSD post-hoc analysis. Non-parametric data was additionally subjected to Kruskal Wallis test followed by multiple pairwise comparison. Significance level for all tests was set for $p < 0.05$. Statistical analysis were performed using SPSS 23.0 software (SPSS, ICN., Chicago, IL).

Supporting Information

Supporting Information is available from the Wiley Online Library or from the author.

Acknowledgements

The authors acknowledge the Spanish Government for financial support through project, co-funded by the EU through European Regional Development Funds, and FPI scholarship of JMS. They also thank the Generalitat the Catalunya for funding through project 2017SGR-1165. MPG acknowledges the o by the Generalitat de Catalunya.

Received: ((will be filled in by the editorial staff))
Revised: ((will be filled in by the editorial staff))
Published online: ((will be filled in by the editorial staff))

References

[1] K. Hu, B. R. Olsen, *J. Clin. Invest.* **2016**, *126*, 509.

[2] A. P. Kusumbe, S. K. Ramasamy, R. H. Adams, *Nature* **2014**, *507*, 323.

[3] S. Stegen, N. van Gastel, G. Carmeliet, *Bone* **2015**, *70*, 19.

[4] H. Mayer, H. Bertram, W. Lindenmaier, T. Korff, H. Weber, H. Weich, *J. Cell. Biochem.* **2005**, *95*, 827.

[5] S. Javerzat, P. Auguste, A. Bikfalvi, *Trends Mol. Med.* **2002**, *8*, 483.

[6] J.-M. Kim, H.-I. Shin, S.-S. Cha, C. S. Lee, B. S. Hong, S. Lim, H.-J. Jang, J. Kim, Y. R. Yang, Y.-H. Kim, S. Yun, G. Rijal, W. Lee-Kwon, J. K. Seo1, Y. S. Gho, S. H. Ryu, E.-M. Hur, P.-G. Suh, *Nat. Commun.* **2012**, *3*, 1296.

[7] M. Raida, A. C. Heymann, C. Günther, D. Niederwieser, *Int. J. Mol. Med.* **2006**, *18*, 735.

[8] D. M. Smadja, I. Bièche, J. S. Silvestre, S. Germain, A. Cornet, I. Laurendeau, J. P. Duong-Van-Huyen, J. Emmerich, M. Vidaud, M. Aiach, P. Gaussem, *Arterioscler. Thromb. Vasc. Biol.* **2008**, *28*, 2137.

[9] L. A. Dyer, X. Pi, C. Patterson, *Trends Endocrinol. Metab.* **2014**, *25*, 472.

[10] A. M. Parfitt, *Bone* **2000**, *26*, 319.

[11] A. Barba, Y. Maazouz, A. Diez-Escudero, K. Rappe, M. Espanol, E. B. Montufar, C. Öhman-Mägi, C. Persson, P. Fontecha, M.-C. Manzanares, J. Franch, M.-P. Ginebra, *Acta Biomater.* **2018**, DOI: 10.1016/j.actbio.2018.09.003. [ahead of print]

[12] A. Barba, A. Diez-Escudero, Y. Maazouz, K. Rappe, M. Espanol, E. B. Montufar, M. Bonany, J. M. Sadowska, J. Guillem-Marti, C. Öhman-Mägi, C. Persson, M.-C. Manzanares, J. Franch, M.-P. Ginebra, *ACS Appl. Mater. Interfaces* **2017**, *9*, 41722.

[13] C. Danoux, D. Pereira, N. Döbelin, C. Stähli, J. Barralet, C. van Blitterswijk, P. Habibovic, *Adv. Healthc. Mater.* **2016**, *5*, 1775.

[14] C. Danoux, L. Sun, G. Koçer, Z. T. Birgani, D. Barata, J. Barralet, C. Van Blitterswijk, R. Truckenmüller, P. Habibovic, *Adv. Mater.* **2016**, *28*, 1803.

[15] X. Xiao, W. Wang, D. Liu, H. Zhang, P. Gao, L. Geng, Y. Yuan, J. Lu, Z. Wang, *Sci. Rep.* **2015**, *5*, 9409.

[16] W. Chen, W. Thein-Han, M. D. Weir, Q. Chen, H. H. K. Xu, *Dent. Mater.* **2014**, *30*, 535.

[17] Z. S. Patel, S. Young, Y. Tabata, J. A. Jansen, M. E. K. Wong, A. G. Mikos, *Bone* **2008**, *43*, 931.

[18] H. X. Zhang, X. P. Zhang, G. Y. Xiao, Y. Hou, L. Cheng, M. Si, S. S. Wang, Y. H. Li, L. Nie, *Mater. Sci. Eng. C* **2016**, *60*, 298.

[19] J. Barralet, U. Gbureck, P. Habibovic, E. Vorndran, C. Gerard, C. J. Doillon, *Tissue Eng. Part A* **2009**, *15*, 1601.

[20] S. Bose, G. Fielding, S. Tarafder, A. Bandyopadhyay, *Trends Biotechnol.* **2013**, *31*, 594.

[21] W. Thein-Han, H. H. K. Xu, *Tissue Eng. Part A* **2013**, *19*, 1675.

[22] M. M. L. Deckers, R. L. van Bezooijen, G. van der Horst, J. Hoogendam, C. van der Bent, S. E. Papapoulos, C. W. G. M. Löwik, *Endocrinology* **2002**, *143*, 1545.

[23] H. von Schroeder, C. Veillette, J. Payandeh, A. Qureshi, J. N. Heersche, *Bone* **2003**, *33*, 673.

[24] S. J. Bidarra, C. C. Barrias, M. A. Barbosa, R. Soares, J. Amédée, P. L. Granja, *Stem Cell Res.* **2011**, *7*, 186.

[25] J. Ma, J. J. J. P. van den Beucken, F. Yang, S. K. Both, F.-Z. Cui, J. Pan, J. A. Jansen, *Tissue Eng. Part C. Methods* **2011**, *17*, 349.

[26] Y. Kang, S. Kim, M. Fahrenholtz, A. Khademhosseini, Y. Yang, *Acta Biomater.* **2013**, *9*, 4906.

[27] W. Sun, A. Motta, Y. Shi, A. Seekamp, H. Schmidt, S. N. Gorb, C. Migliaresi, S. Fuchs, *Biomed. Mater.* **2016**, *11*, 35009.

[28] T. O. Pedersen, A. L. Blois, Y. Xue, Z. Xing, Y. Sun, A. Finne-Wistrand, J. B. Lorens, I. Fristad, K. N. Leknes, K. Mustafa, *Stem Cell Res. Ther.* **2014**, *5*, 23.

[29] X. Liu, W. Chen, C. Zhang, W. Thein-Han, K. Hu, M. A. Reynolds, C. Bao, P. Wang, L. Zhao, H. H. K. Xu, *Tissue Eng. Part A* **2017**, *23*, 546.

[30] A. Bouacida, P. Rosset, V. Trichet, F. Guilloton, N. Espagnolle, T. Cordonier, D. Heymann, P. Layrolle, L. Sensébé, F. Deschaseaux, *PLoS One* **2012**, *7*, e48648.

[31] K. Janeczek Portalska, A. Leferink, N. Groen, H. Fernandes, L. Moroni, C. van

Blitterswijk, J. de Boer, *PLoS One* **2012**, *7*, e46842.

[32] J. König, B. Huppertz, G. Desoye, O. Parolini, J. D. Fröhlich, G. Weiss, G. Dohr, P. Sedlmayr, I. Lang, *Stem Cells Dev.* **2012**, *21*, 1309.

[33] C. Knabe, F. C. Driessens, J. a Planell, R. Gildenhaar, G. Berger, D. Reif, R. Fitzner, R. J. Radlanski, U. Gross, *J. Biomed. Mater. Res.* **2000**, *52*, 498.

[34] J. Gustavsson, M. P. P. Ginebra, E. Engel, J. Planell, *Acta Biomater.* **2011**, *7*, 4242.

[35] J. Gustavsson, M. P. Ginebra, J. Planell, E. Engel, *J. Mater. Sci. Mater. Med.* **2012**, *23*, 2509.

[36] J.-M. Sadowska, J. Guillem-Marti, E. B. Montufar, M. Espanol, M.-P. Ginebra, *Tissue Eng. Part A* **2017**, *23*, 1297.

[37] N. Vandecandelaere, C. Rey, C. Drouet, *J. Mater. Sci. Mater. Med.* **2012**, *23*, 2593.

[38] S. Cazalbou, D. Eichert, X. Ranz, C. Drouet, C. Combes, M. F. Harmand, C. Rey, *J. Mater. Sci. Mater. Med.* **2005**, *16*, 405.

[39] J. M. Sadowska, F. Wei, J. Guo, J. Guillem-Marti, M.-P. Ginebra, Y. Xiao, *Biomaterials* **2018**, *181*, 318.

[40] G. Ciapetti, G. Di Pompo, S. Avnet, D. Martini, A. Diez-Escudero, E. B. Montufar, M.-P. Ginebra, N. Baldini, *Acta Biomater.* **2017**, *50*, 102.

[41] J. M. Sadowska, J. Guillem-Marti, M. Espanol, C. Stähli, N. Döbelin, M.-P. Ginebra, *Acta Biomater.* **2018**, *76*, 319.

[42] A. Peng, T. Wu, C. Zeng, D. Rakheja, J. Zhu, T. Ye, J. Hutcheson, N.D. Vaziri, Z. Liu, C. Mohan, X.J. Zhou, *PLoS One*. **2011**, *6*, e23268.

[43] G. S. Di Marco, M. Hausberg, U. Hillebrand, P. Rustemeyer, W. Wittkowski, D. Lang, H. Pavenstädt, *Am. J. Physiol. Renal Physiol.* **2008**, *294*, F1381.

[44] C. Xu, F. Yang, S. Wang, S. Ramakrishna, *J. Biomed. Mater. Res. - Part A* **2004**, *71*, 154.

[45] J. A. Mmaier, D. Bernardini, Y. Rayssiguier, A. Mazur, *Biochimica et Biophysica Acta*

2004, *1689*, 6.

[46] K. Sternberg, M. Gratz, K. Koeck, J. Mostertz, R. Begunk, M. Loebler, B. Semmling, A. Seidlitz, P. Hildebrandt, G. Homuth, N. Grabow, C. Tuemmler, W. Weitschies, K. P. Schmit, H. Kroemer, *J Biomed Mater Res Part B* **2012**, *100B*, 41.

[47] E. Engel, S. Del Valle, C. Aparicio, G. Altankov, L. Asin, J. a Planell, M.-P. Ginebra, *Tissue Eng. Part A* **2008**, *14*, 1341.

[48] Y. K. Y. K. Liu, Q. Z. Q. Z. Lu, R. Pei, H. J. H. J. Ji, G. S. G. S. Zhou, X. L. X. L. Zhao, R. K. R. K. Tang, M. Zhang, *Biomed. Mater.* **2009**, *4*, 025004.

[49] S. Fuchs, X. Jiang, H. Schmidt, E. Dohle, S. Ghanaati, C. Orth, A. Hofmann, A. Motta, C. Migliaresi, C. J. Kirkpatrick, *Biomaterials* **2009**, *30*, 1329.

[50] G. S. Di Marco, M. König, C. Stock, A. Wiesinger, U. Hillebrand, S. Reiermann, S. Reuter, S. Amler, G. Köhler, F. Buck, M. Fobker, P. Kümpers, H. Oberleithner, M. Hausberg, D. Lang, H. Pavenstädt, M. Brand, *Kidney Int.* **2013**, *83*, 213.

[51] H. Peng, A. Usas, A. Olshanski, A. M. Ho, B. Gearhart, G. M. Cooper, J. Huard, *J. Bone Miner. Res.* **2005**, *20*, 2017.

[52] N. Akeno, J. Robins, M. Zhang, M. F. Czyzyk-Krzeska, T. L. Clemens, *Endocrinology* **2002**, *143*, 420.

[53] K. Eldesoqi, C. Seebach, C. Nguyen Ngoc, S. Meier, C. Nau, A. Schaible, I. Marzi, D. Henrich, *PLoS One* **2013**, *8*, e79058.

[54] A. Aguirre, A. González, M. Navarro, Ó. Castaño, J. A. Planell, E. Engel, *Eur. Cells Mater.* **2012**, *24*, 90.

[55] R. Olivares-Navarrete, S. L. Hyzy, R. A. Gittens, J. M. Schneider, D. A. Haithcock, P. F. Ullrich, P. J. Slosar, Z. Schwartz, B. D. Boyan, W. H. Coulter, *Spine J.* **2013**, *13*, 1563.

[56] N. Ferrara, H.-P. Gerber, J. LeCouter, *Nat. Med.* **2003**, *9*, 669.

[57] S. Koch, L. Claesson-Welsh, *Cold Spring Harb. Perspect. Med.* **2012**, *2*, 1.

[58] D. Salani, G. Taraboletti, L. Rosanò, V. Di Castro, P. Borsotti, R. Giavazzi, A. Bagnato, *Am. J. Pathol.* **2000**, *157*, 1703.

[59] E. E. Golub, G. Harrison, a G. Taylor, S. Camper, I. M. Shapiro, *Bone Miner.* **1992**, *17*, 273.

[60] H. I. Roach, *Cell Biol. Int.* **1994**, *18*, 617.

[61] S. Vasseur, S. Afzal, J. Tardivel-Lacombe, D. S. Park, J. L. Iovanna, T. W. Mak, *Proc. Natl. Acad. Sci.* **2009**, *106*, 1111.

[62] J. Hoogendam, C. V. a N. D. E. R. Bent, S. E. Papapoulos, C. W. G. M. Lo, *Endocrinology* **2014**, *143*, 1545.

[63] U. Bulnheim, P. Müller, H. Neumann, K. Peters, R. E. Unger, C. J. Kirkpatrick, J. Rychly, *J. Tissue Eng. Regen. Med.* **2014**, *8*, 831.

[64] R. McBeath, D. M. Pirone, C. M. Nelson, K. Bhadriraju, C. S. Chen, *Dev. Cell* **2004**, *6*, 483.

[65] K. A. Kilian, B. Bugarija, B. T. Lahn, M. Mrksich, *Proc. Natl. Acad. Sci. U. S. A.* **2010**, *107*, 4872.

[66] F. Villars, B. Guillotin, T. Amédée, S. Dutoya, L. Bordenave, R. Bareille, J. Amédée, *Am. J. Physiol. Cell Physiol.* **2002**, *282*, C775.

[67] D. Kaigler, P. H. Krebsbach, E. R. West, K. Horger, Y.-C. Huang, D. J. Mooney, *FASEB J.* **2005**, *19*, 665.

[68] M. P. Ginebra, E. Fernandez, E. a. P. A. De Maeyer, R. M. H. M. Verbeeck, M. G. G. Boltong, J. Ginebra, F. C. Driessens, J. A. A. Planell, *J. Dent. Res.* **1997**, *76*, 905.

[69] M. Espanol, R. A. Perez, E. B. Montufar, C. Marichal, A. Sacco, M. P. Ginebra, *Acta Biomater.* **2009**, *5*, 2752.

[70] F. H. Chung, *J. Appl. Crystallogr.* **1974**, *7*, 519.

[71] A. Diez-Escudero, M. Espanol, S. Beats, M.-P. Ginebra, *Acta Biomater.* **2017**, *60*, 81.

[72] A. Aguirre, A. González, J. A. Planell, E. Engel, *Biochem. Biophys. Res. Commun.*

2010, *393*, 156.

[73] A. Aguirre, J. A. Planell, E. Engel, *Biochem. Biophys. Res. Commun.* **2010**, *400*, 284.

[74] J. Stern, W. H. P. Lewis, *Clin. Chim. Acta* **1957**, *2*, 576.

[75] J. Gitelman, *Anal. Biochem.* **1967**, *18*, 521.

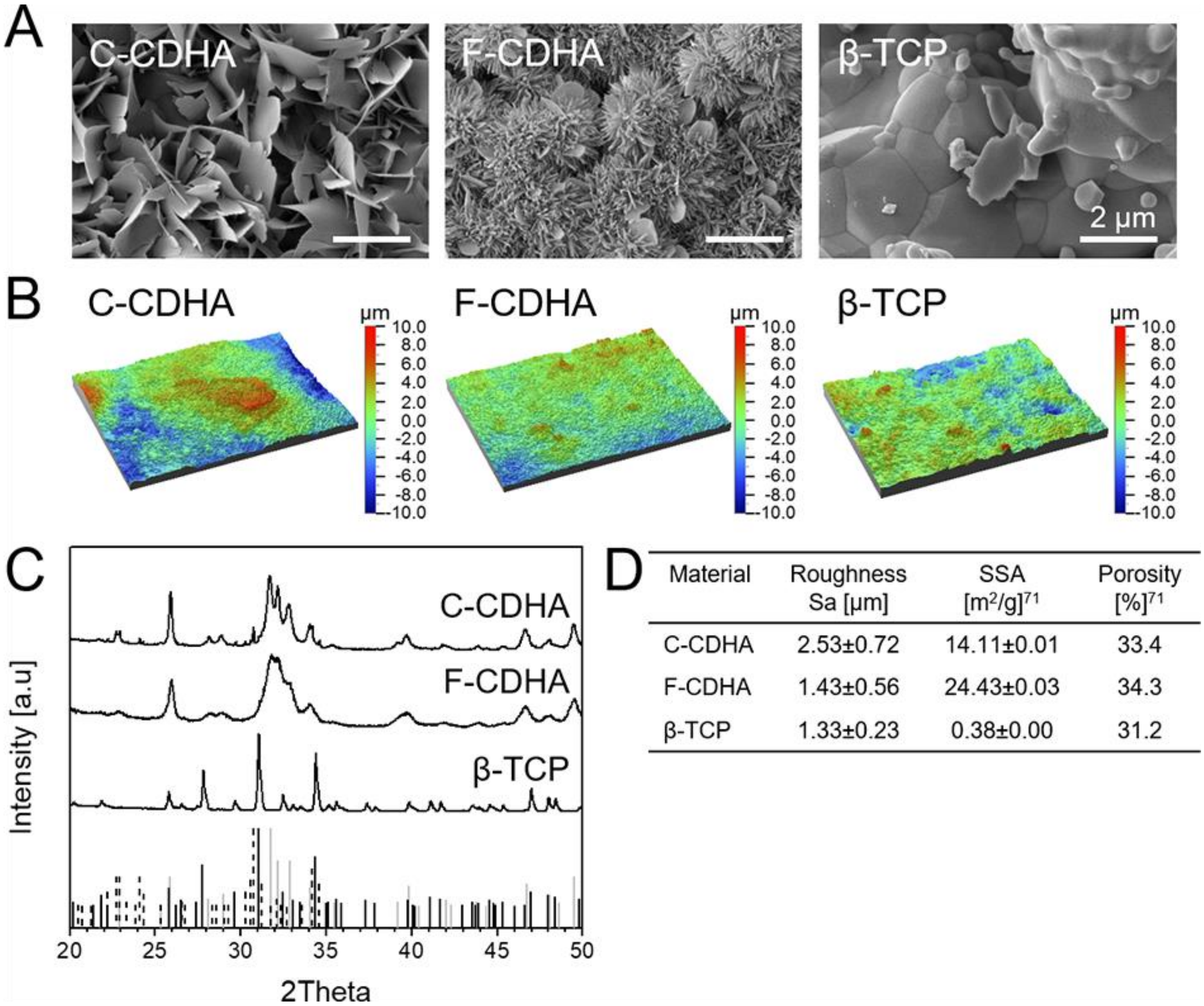

Material	Roughness Sa [µm]	SSA [m²/g][71]	Porosity [%][71]
C-CDHA	2.53±0.72	14.11±0.01	33.4
F-CDHA	1.43±0.56	24.43±0.03	34.3
β-TCP	1.33±0.23	0.38±0.00	31.2

Figure 1. Physicochemical characterization of CaPs A) SEM micrographs of surface morphology. Scale bare denotes 2 µm. B) Optical interferometry images of C-CDHA, F-CDHA and β-TCP. C) XRD patterns of the different calcium phosphate substrates. The vertical lines represent the patterns of HA (JCPDS 82-1943), α-TCP (JCPDS 09-0348) and β-TCP (JCPDS 70-2065) from the Joint Committee on powder Diffraction Standards. D) Values of roughness, specific surface area (SSA) and total porosity.[71]

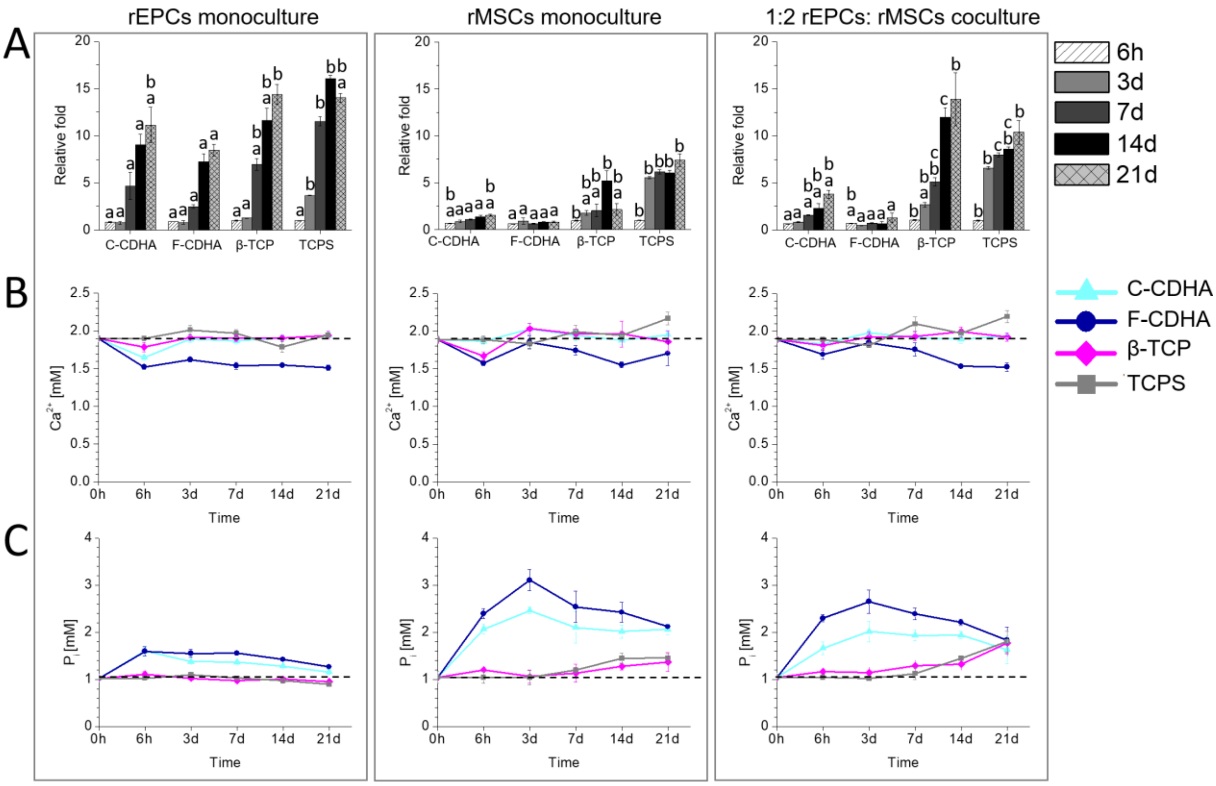

Figure 2. A) Proliferation of monocultured rEPCs, monocultured rMCSs and cocultured cells with ratio 1:2 of rEPCs and rMSCs on various CaPs. Cell numbers were quantified at 6 hours, 3 days, 7 days, 14 days and 21 days (n=6). The values were expressed as relative fold change compared to cell number obtained on corresponding TCPS at 6 hours. In all graphs, the same letter (a, b or c) indicate groups with no statistically significant differences ($p > 0.05$) at specific time point. B) Calcium concentration in EGM-2 MV medium in presence of cells (n=6). C) Phosphate concentration in EGM-2 MV medium in presence of cells (n=6).

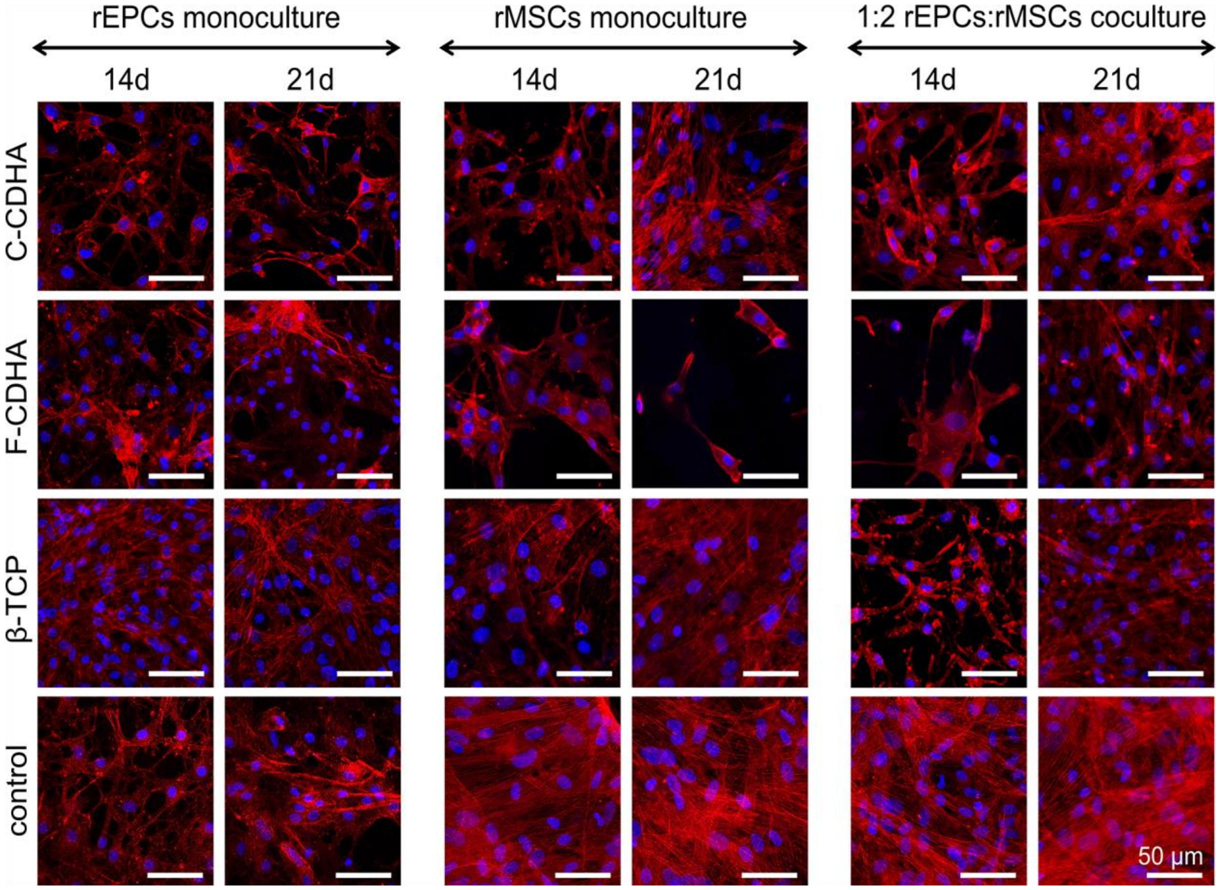

Figure 3. Merged fluorescence images of monocultured rEPCs, monocultured rMSCs and cocultured cells with ratio 1:2 of rEPCs and rMSCs on various CaPs. Cells were stained for F-actin (red) and nuclei (blue). The images were acquired at 14 days and 21 days of cell culture. The cells seeded on glass coverslip were used as a control. Scale bar denotes 50 μm.

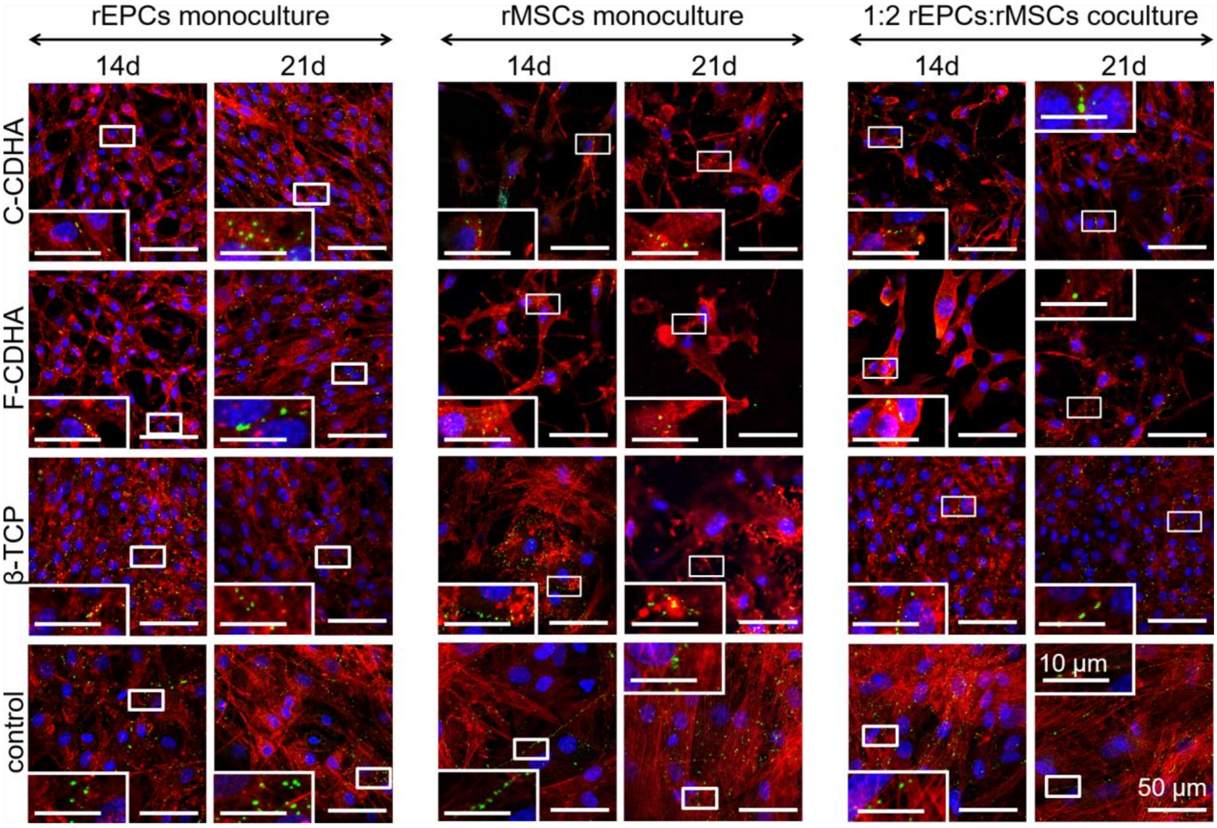

Figure 4. Merged fluorescence images of monocultured rEPCs, monocultured rMSCs and cocultured cells with ratio 1:2 of rEPCs and rMSCs on C-CDHA, F-CDHA and β-TCP at 14 and 21 days of cell culture. Cells were stained for Connexin43 (green), F-actin (red) and nuclei (blue). Scale bars denote 50 μm in the main images and 10 μm in the insets.

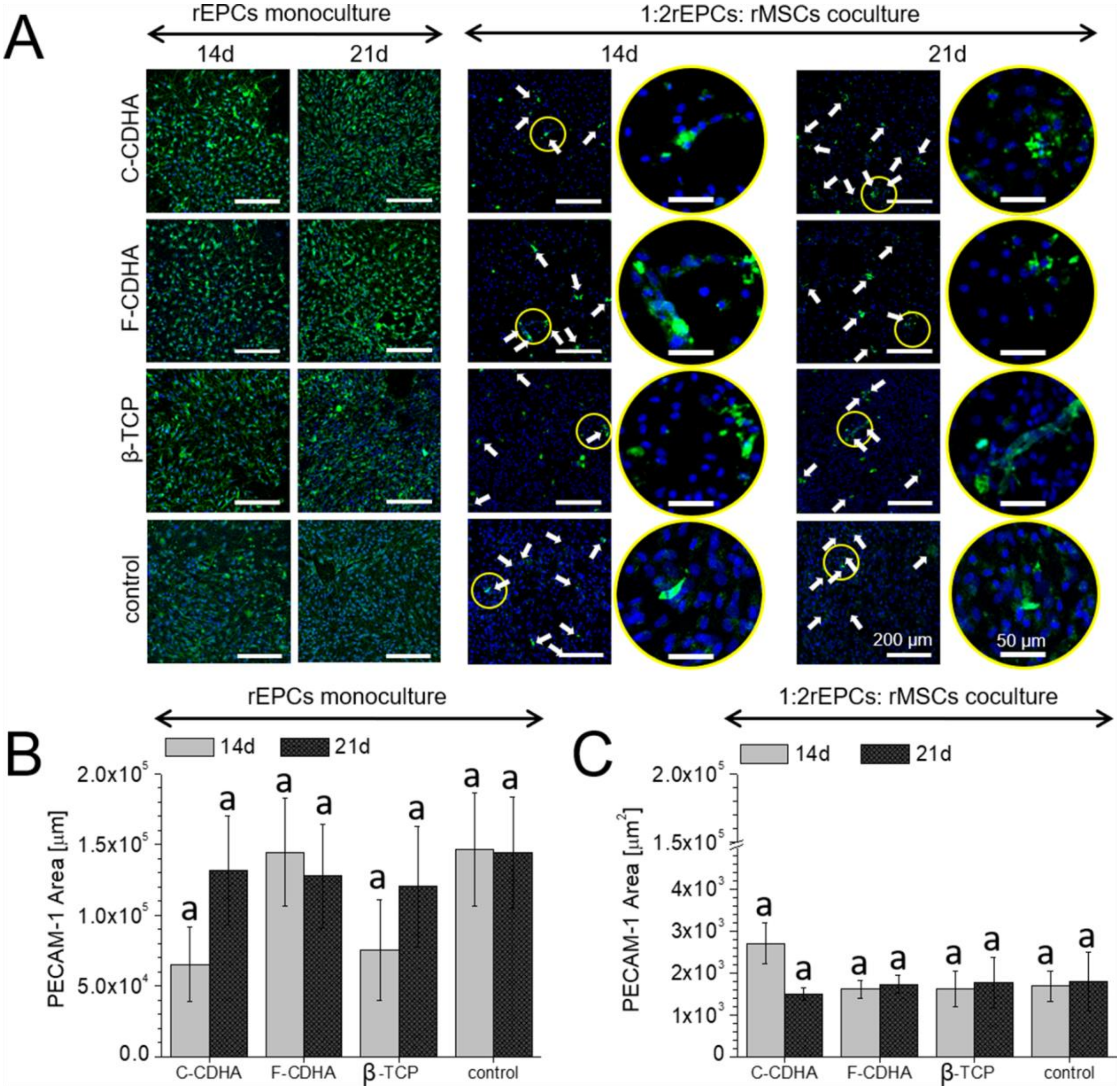

Figure 5. A) Merged fluorescence images of monocultured rEPCs and cocultured cells at ratio 1:2 of rEPCs and rMSCs on C-CDHA, F-CDHA and β-TCP at 14 and 21 days of cell culture. Cells were stained for PECAM-1 (green) and nuclei (blue). For coculture images, cells stained with both PECAM-1 and nuclei correspond to rEPCs whilst cells without PECAM-1 staining represent rMSCs. Scale bar denotes 200 μm for the main images and 50 μm for magnified images. B) Semiquantitative evaluation of area of PECAM-1 staining in monoculutred rEPCs on CaPs at 14 and 21 days (n=10). C) Semiquantitative evaluation of the area of PECAM-1 staining in cocultured 1:2 rEPCs and rMSCs on CaPs at 14 and 21 days (n=10). In graphs B and C, the same letter indicates groups with no statistically significant differences ($p > 0.05$) at specific time point.

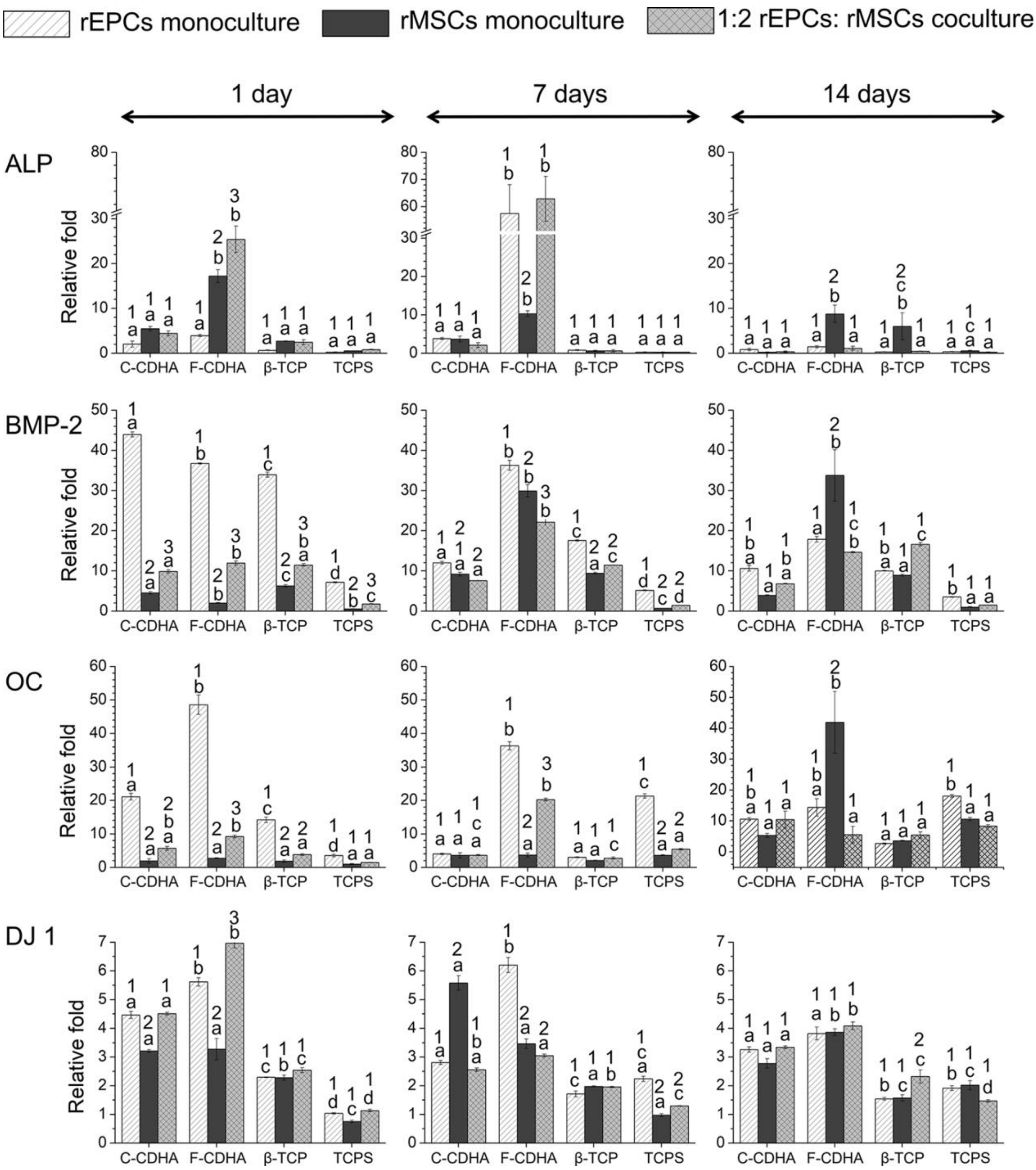

Figure 6. Gene expression of osteogenic markers in monocultured rEPCs, monocultured rMSCs and coculture on three calcium phosphate substrates (n=6). Expressions levels were determined by quantitative real time RT-PCR, normalised versus monocultured rMSCs on TCPS at 1 day and displayed relative to their housekeeping gene. In all graphs, the same letter (a, b, c or d) indicates no statistically significant differences ($p > 0.05$) between substrates for each specific cell culture condition (rEPCs monoculture, rMSCs monoculture, rEPCs: rMSCs

coculture). The same number (1, 2 or 3) indicates no statistically significant differences (p > 0.05) between cell culture conditions for each substrate (C-CDHA, F-CDHA, β-TCP, TCPS).

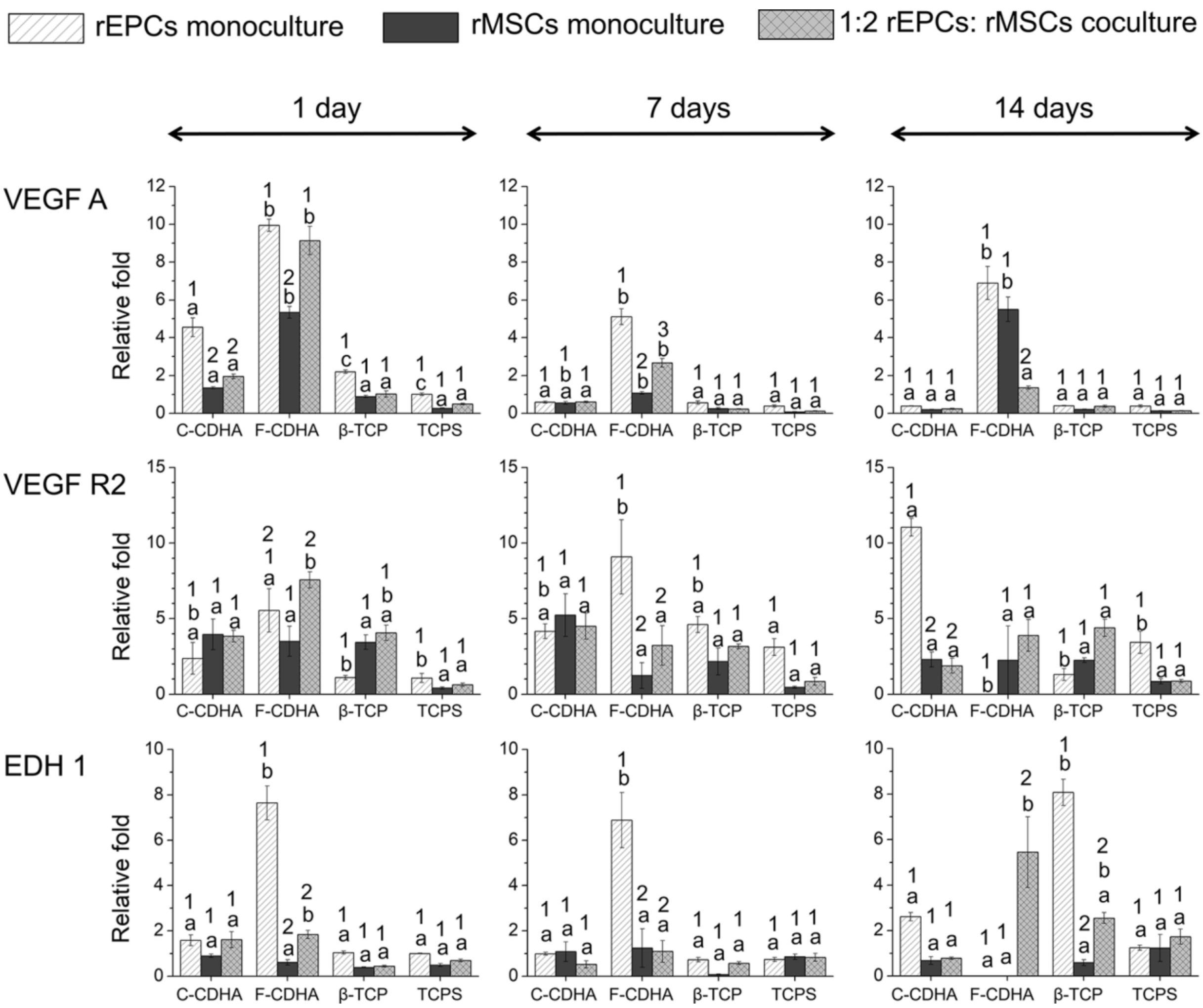

Figure 7. Gene expression of angiogenic markers in monocultured rEPCs, monocultured rMSCs and coculture on three calcium phosphate substrates (n=6). Expressions levels were determined by quantitative real time RT-PCR, normalised versus monocultured rEPCs on TCPS at 1 day. and displayed relative to their housekeeping gene. In all graphs, the same letter (a, b, c or d) indicates no statistically significant differences (p > 0.05) between substrates for each specific cell culture condition (rEPCs monoculture, rMSCs monoculture, rEPCs: rMSCs coculture). The same number (1, 2 or 3) indicates no statistically significant differences (p > 0.05) between cell culture conditions for each substrate (C-CDHA, F-CDHA, β-TCP, TCPS).

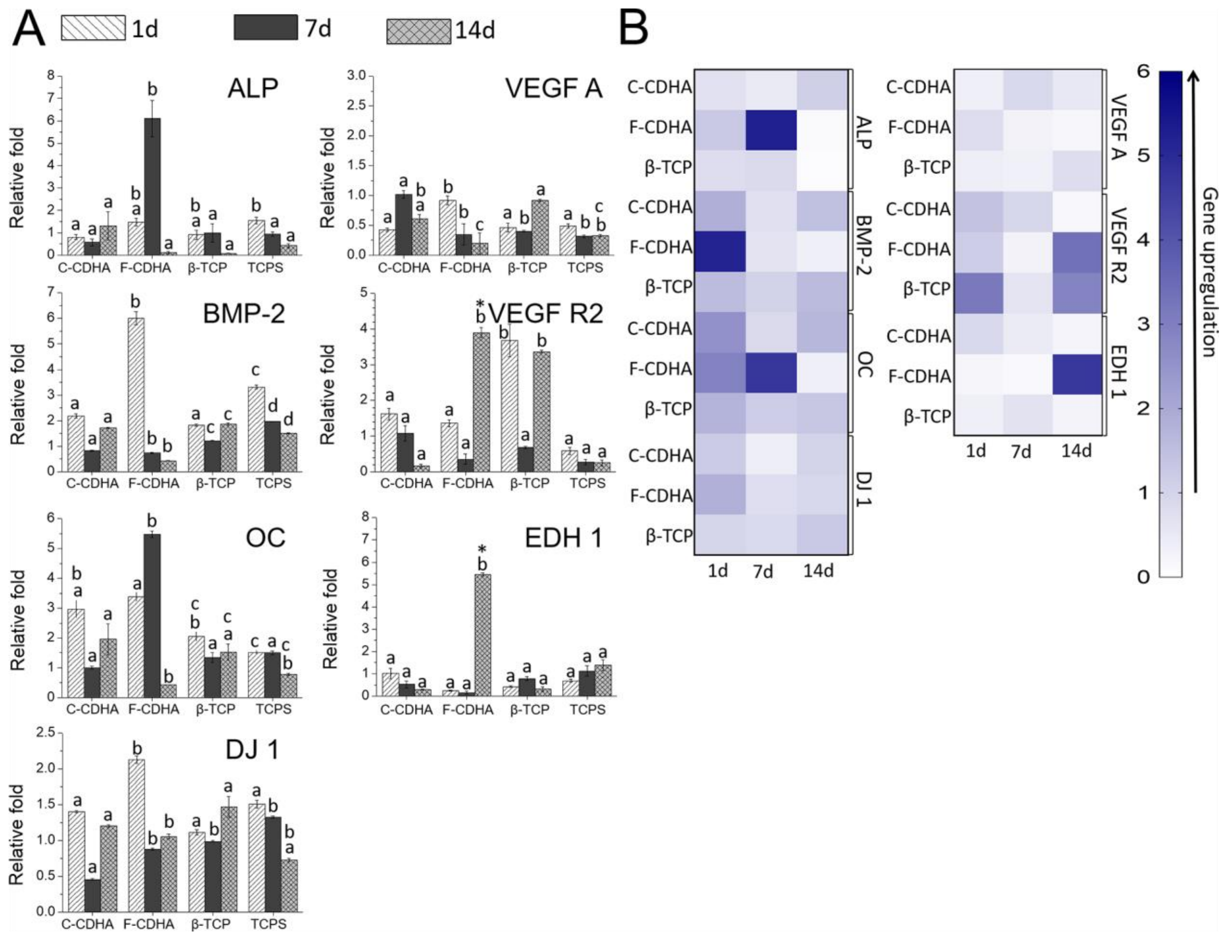

Figure 8. A) Effect of culturing both rEPCS and rMSCs on the gene expression of osteogenesis and angiogenesis related genes compared to monocultured cells (n=6). In order to see either specific gene is upregulated in coculture system the gene expression was normalised versus gene expression in monocultured rMSCs or monocultured rEPCs for osteogenic (ALP, BMP-2, OC, DJ 1) or angiogenic (VEGF A, VEGF R2, EDH 1) genes, respectively. For samples where gene expression in monoculture was not detected the mean value obtained in coculture was plotted (*). In all graphs, the same letter (a, b, c or d) indicates no statistically significant differences ($p > 0.05$) between substrates for each specific time point. B) Heat map of gene upregulation in coculture system.

Click here to access/download
Supporting Information
Sadowska AHM Supporting information.docx

Click here to access/download
Production Data
Sadowska AHM fv manuscript-production data.doc

Short summary

Click here to access/download
Production Data
Sadowska AHM summary and ToC.docx

Click here to access/download
Production Data
Sadowska AHM Table of contents.tif

Click here to access/download
Production Data
Sadowska AHM Supporting information-production data.docx

Figure 1

Click here to access/download
Production Data
FIGURE 1.tif

Figure 2

Click here to access/download
Production Data
FIGURE 2.tif

Figure 2

Click here to access/download
Production Data
FIGURE 3.tif

Figure 4

Click here to access/download
Production Data
FIGURE 4.tif

Figure 5

Click here to access/download
Production Data
FIGURE 5.tif

Figure 6

Click here to access/download
Production Data
FIGURE 6.tif

Figure 7

Click here to access/download
Production Data
FIGURE 7.tif

Figure 8

Click here to access/download
Production Data
FIGURE 8.tif